Design of Low Band Gap Polymers Employing Density Functional Theory—Hybrid Functionals Ameliorate Band Gap Problem

U. SALZNER,[1] J. B. LAGOWSKI,[2] P. G. PICKUP,[1] and R. A. POIRIER[1]

[1]*Department of Chemistry, Memorial University of Newfoundland, St. John's, NF A1B 3X7, Canada*
[2]*Department of Physics and Physical Oceanography, Memorial University of Newfoundland, St. John's, NF A1B 3X7, Canada*

ABSTRACT: Band gaps in solids and excitation energies in finite systems are underestimated significantly if estimated from differences between eigenvalues obtained within the local spin density approximation (LSDA). In this article we present results on 20 small- and medium-sized π-systems which show that HOMO−LUMO energy differences obtained with the B3LYP, B3P86, and B3PW91 functionals are in good agreement with vertical excitation energies from UV-absorption spectra. The improvement is a result of the use of the exact Hartree−Fock exchange with hybrid methods. Negative HOMO energies and negative LUMO energies do not provide good estimates for IPs and EAs. In contrast to Hartree−Fock theory, where IPs are approximated well and EAs are given poorly, DFT hybrid methods underestimate IPs and EAs by about the same amount. LSDA yields reasonable EAs but poor IPs.   © 1997 John Wiley & Sons, Inc.   *J Comput Chem* **18**: 1943−1953, 1997

Keywords: conducting polymers; band gap problem; density functional theory; hybrid functionals; ionization potentials and electron affinities

Introduction

The energy gap between valence and conduction band of a polymer is related to the lowest allowed excitation energy of its monomer units and to the bandwidth resulting from the overlap between the monomer orbitals (Fig. 1).[1,2] To design a low band gap polymer it is thus desirable to start with monomer units with small excitation energies. Systematic investigations of trends in excitation energies depending on structure and substitution can be carried out on monomers and oligomers before performing time-extensive band structure calculations.

There are, in principle, three ways to obtain excitation energies. The most obvious one is to calculate the energy of the ground and the excited state explicitly and to take the energy difference. For excited states that cannot be described by single determinant wave functions both dynamic and nondynamic correlation effects are important. Highly correlated wave functions,[3,4] or better, multireference perturbation theory, is necessary to obtain reasonable excitation energies.[5,6] For screening large numbers of big systems such high level calculations are not practical.

An alternative method is to compute the excitation energy as the difference between ionization potential (IP) and electron affinity (EA).[7] In solid state physics, IPs and EAs are referred to as quasiparticle energies. Quasiparticle energies can be calculated to high accuracy with Green's functions theory, but this is extremely demanding computationally.[8,9] In finite systems, accurate IPs and EAs
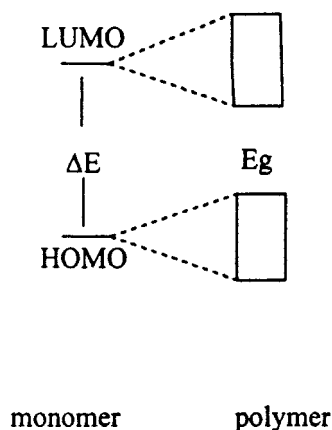
are obtained as energy differences between the cation or anion and the neutral system. Because energies of anions are notoriously difficult to calculate, this method is also not feasible for creation of large data sets.

The third method is to estimate excitation energies as HOMO−LUMO energy differences. This corresponds to a frozen orbital approximation since the ground state orbitals are used to estimate the excited state energy. For the conjugated π-systems considered here, this crude approach is justified, because it has been established[4,10] that the lowest singlet transition (V ← N) is essentially a valence-like π−π^* transition. In the framework of Hartree−Fock (HF) theory, the frozen orbital approximation leads to significant overestimation of the gaps of finite and infinite systems because the LUMO energy calculated for the neutral systems gives the electron affinity of the corresponding anion rather than that of the neutral system.[11] The negative HOMO energy of HF theory, in contrast, is known to correlate very well with vertical IPs (Koopman's theorem).[12] In spite of its shortcomings, the frozen orbital approximation is the only practical method if a large number of systems or very large molecules have to be investigated. Band gaps obtained from band structure calculations for solids are analogous to HOMO−LUMO energy differences of molecules.

Many modern solid state programs use density functional theory (DFT) in connection with the Car−Parinello method because high quality results can be obtained very efficiently using fast Fourier transform techniques.[13,14] DFT is also very attractive for calculations on finite systems because even the lowest level of DFT—the local spin density approximation (LSDA)—includes some electron correlation. This is extremely important for the design of conducting organic polymers which have extended π-systems. Properties like bond length alternation are very sensitive to electron correlation and cannot be predicted with sufficient accuracy at the HF level.[15−17] Bond length alternation in turn has a strong influence on the band gap.[18] There is thus a vital interest to use DFT methods for band structure calculations and for the estimation of excitation energies of monomers and oligomers.

The use of DFT one-electron energy differences to estimate excitation energies, however, is still a matter of debate.[7−9,19−27] In contrast to Hartree−Fock theory, where one-electron functions are used to minimize the energy directly, orbitals in density functional theory are used to construct the correct

FIGURE 1. Relationship between HOMO−LUMO levels of finite and band gaps of infinite systems.

electron density. The energies of these orbitals, therefore, have no obvious physical meaning.[21, 27] Band structure calculations on various semiconductors have nonetheless shown that, although LSDA eigenvalue differences underestimate the band gap compared to experiment, the shift is almost vertical and very systematic.[26] Numerous theoretical studies have been published investigating the source of the so-called band gap problem.[8, 9, 19, 20, 22–24, 26] It has been claimed that the error is caused by the derivative discontinuity in the exchange-correlation functional with respect to the charge density. This derivative discontinuity is inherent in DFT and would also be present if the exact exchange-correlation functional was used. Therefore, it was predicted that the band gap problem would not be overcome in going beyond LSDA. The same argument holds for finite and infinite systems.[26]

In this article we present excitation energies of 20 small- and medium-sized π-systems estimated as one-electron energy differences at the HF and DFT levels with various combinations of exchange and correlation functionals. The results show that inclusion of the exact Hartree–Fock exchange via the hybrid B3LYP, B3P86, and B3PW91 functionals leads to HOMO–LUMO gaps in good agreement with experimental excitation energies.

Methods

A series of even-numbered all-trans-polyenes starting with ethylene, C_2H_4, and ending with $C_{16}H_{18}$ (compounds **1–8**) was fully optimized at the RHF level and with DFT methods employing the Slater (S), Becke 88 (B), and the Becke three-parameter hybrid (B3) exchange functionals in various combinations with the Vosko–Wilk–Nusair (VWN), Lee–Yang–Parr (LYP), Perdew (P86), and Perdew and Wang (PW91) correlation functionals.[28] SVWN is identical to LSDA. B3LYP indicates that Becke's three-parameter hybrid functional is used in combination with the LYP correlation functional. This functional can be expressed as[28]:

$$A \times E_x^{\text{Slater}} + (1 - A) \times E_x^{\text{HF}} + B \times E_x^{\text{Becke}} + C \times E_C^{\text{LYP}} + E_C^{\text{VWN}} \tag{1}$$

B3P86 and B3PW91 are defined analogously and differ only in the use of the respective correlation functional E_C. The values of A, B, and C are 0.80, 0.72, and 0.81 as determined by Becke.[28] The im-

portant difference from the other exchange functionals lies in the exchange part of the functional which incorporates the exact Hartree–Fock exchange with a weight of 20%. $C_{18}H_{20}$ (**9**) and $C_{20}H_{22}$ (**10**) were optimized at B3P86 only.

The calculations were carried out using Stephens/Basch/Krauss ECPs with split valence basis sets augmented with polarization functions on heavy atoms and with the Dunning-95 basis set for first row atoms and Los Alamos ECPs plus double-zeta basis on all other atoms (CEP-31G* and LANL2DZ keywords in G94).[28] B3LYP calculations were also carried out with the 6-31G* basis set to assess the effect of the pseudopotential.

A second set of molecules consisting of cyclic π-systems (Fig. 2) including cyclopentadiene (**11**), furan (**12**), pyrrole (**13**), thiophene (**14**), bithiophene (**15**), terthiophene (**16**), 2,5-bis(2-thienyl)pyridine (**17**), 2,5-bis(1-methyl-2-pyrrolyl)pyridine (**18**), 2,5-bis(2-selenyl)pyridine (**19**), and 2,6-bis(2-thienyl)pyridine (**20**) was optimized at SVWN and
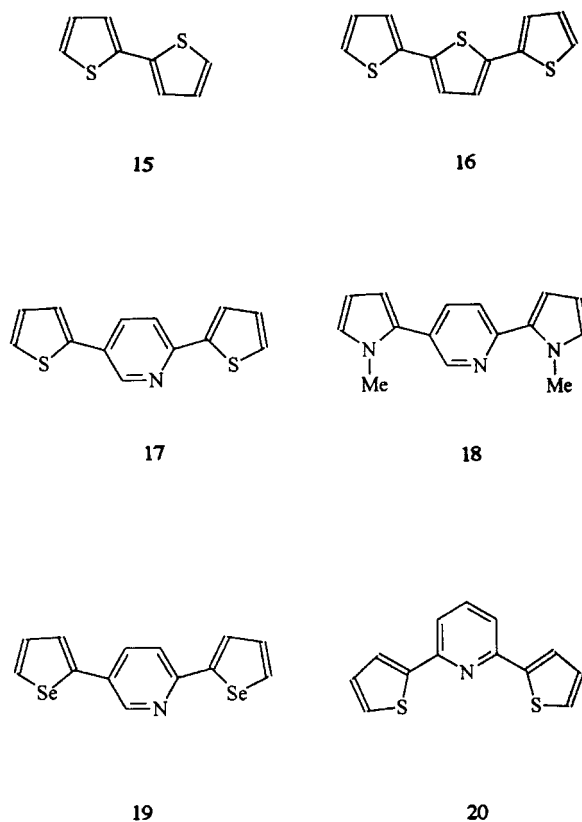

FIGURE 2. Bithiophene **15**, terthiophene **16**, 2,5-bis(2-thienyl)pyridine **17**, 2,5-bis(1-methyl-2-pyrrolyl)pyridine **18**, 2,5-bis(2-selenyl)pyridine **19**, and 2,6-bis(2-thienyl)pyridine **20**.

B3LYP. CEP-31G* and LANL2DZ basis sets were used. For details see Table II. Comparison of results for the systems where both basis sets were tested show that there is little basis set dependence. All calculations were carried out with Gaussian-94.[29]

Although orbitals in density functional theory may have fractional occupations we will refer in the following to the highest quasi fully occupied orbital as the HOMO and to the lowest quasi unoccupied orbital as the LUMO to avoid introducing tedious terminology.

Results

HOMO–LUMO gaps for polyenes **1**–**8** at the RHF, SVWN, BVWN, BLYP, BP86, B3LYP, B3P86, and B3PW91 and for **9** and **10** at B3P86 are listed and compared to peak potentials from UV absorption spectroscopy in Table I. The data are plotted in Figure 3. The theoretical data fall into three groups: As expected the RHF HOMO–LUMO gaps overestimate the excitation energies. The absolute error is 5–6.4 eV. The percent error increases with increasing chain length and amounts to over 100% for $C_{16}H_{18}$. Traditional DFT methods (SVWN, BVWN, BLYP, and BP86) underestimate experimental excitation energies by 1.7–2.3 eV (57% error in $C_{16}H_{18}$). The four different functionals yield almost identical results. Hybrid functionals (B3LYP, B3P86, and B3PW91) yield HOMO–LUMO energy differences in good agreement with experimental excitation energies. Experimental excitation

energies are underestimated by only 0.5–0.8 eV. The absolute error increases slightly with increasing chain length. Like standard DFT functionals the three different hybrid functionals lead to almost identical results. At B3LYP the 6-31G* basis set yields results about 0.1–0.5 eV closer to experiment than CEP-31G*. The advantage, however, seems to decrease with increasing chain length

In Table II, HOMO–LUMO energy differences of aromatic π-systems at the SVWN and the B3LYP levels are compared to experimental excitation energies. In Figure 4, HOMO–LUMO energy differences of polyenes and aromatic systems at SVWN and B3LYP are plotted against experimental excitation energies. The straight line indicates ideal one-to-one correspondence between theory and experiment. B3LYP gaps are shifted vertically from SVWN gaps toward the experimental values. B3LYP thus corrects the systematic underestimation of the gaps at SVWN. In contrast to the simple polyenes, where DFT gaps are consistently too low, gaps of aromatic systems may be either too high or too low. The agreement between theory and experiment is, excellent, however, and shows that the good correlation between DFT HOMO–LUMO energy differences and experimental excitation energies is not restricted to relatively simple polyenes.

Ionization potentials obtained as negative HOMO energies at RHF and various DFT levels are given in Table III and are plotted against chain length in Figure 5. Also included are IPs calculated explicitly as energy differences between the cation and neutral system at B3LYP/CEP-31G*. Experi-

TABLE I.
HOMO–LUMO Energy Differences of Polyenes at Various Theoretical Levels Using the CEP-31G* Basis Set Compared to Vertical Excitation Energies from UV-Absorption Spectroscopy (in Electron Volts).

Species	RHF	SVWN	BVWN	BLYP	BP86	B3LYP	B3LYP 6-31G*	B3P86	B3PW91	Exp.
C_2H_4	14.00	5.44	5.44	5.37	5.44	7.19	7.77	7.28	7.27	7.65[a]
C_4H_6	11.65	3.73	3.76	3.71	3.74	5.31	5.62	5.35	5.34	5.92[b]
C_6H_8	10.29	2.82	2.87	2.90	2.84	4.26	4.49	4.28	4.28	4.95[c]
C_8H_{10}	9.43	2.28	2.32	2.29	2.29	3.61	3.79	3.62	3.62	4.41[d]
$C_{10}H_{12}$	8.86	1.90	1.95	1.93		3.17	3.32	3.17		3.71[e]
$C_{12}H_{14}$	8.45	1.64	1.69	1.67		2.84	2.98	2.84		3.41[e]
$C_{14}H_{16}$	8.15	1.44		1.47		2.60	2.72	2.59		3.18[e]
$C_{16}H_{18}$	7.94	1.29	1.34	1.32	1.31	2.40	2.52	2.39	2.40	3.02[e]
$C_{18}H_{20}$								2.24		2.82[e]
$C_{20}H_{22}$								2.11		2.77[e]

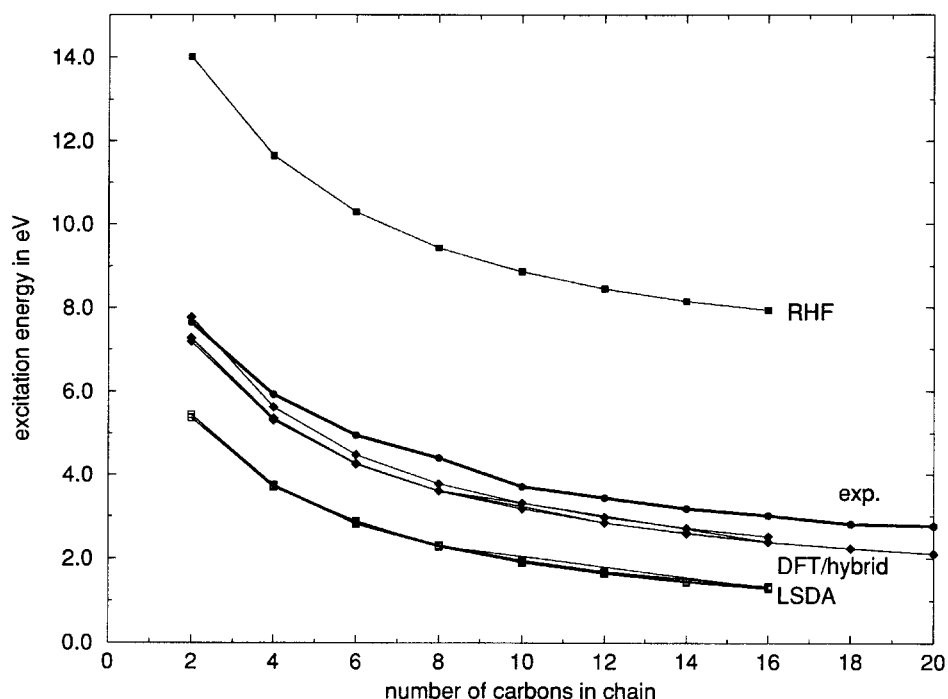[a] Ref. 31, [b] ref. 32, [c] ref. 33, [d] ref. 34, [e] ref. 35.

FIGURE 3. Theoretical HOMO–LUMO gaps and experimental excitation energies for **1–10**.

mental IPs are given where available. RHF IPs obtained according to Koopman's theorem agree well with experimental values for ethene through octatetraene. The experimental values are underestimated by 0.4–0.6 eV. Explicit calculation of IPs as the difference between the cation and neutral species energies with B3LYP leads to similar

agreement with experiment for ethene through octatetraene although the agreement seems to deteriorate for larger systems.

IPs obtained as negative HOMO energies with DFT methods are consistently too low and differ considerably for different functionals. Slater and Becke exchange lead to very similar HOMO ener-

TABLE II.
HOMO–LUMO Energy Differences of Aromatic π-Systems 11–20 at B3LYP / CEP-31G* Compared to Vertical Excitation Energies from UV-Absorption Spectroscopy (in Electron Volts).

	SVWN		B3LYP			
	LANL2DZ	CEP-31G*	LANL2DZ	CEP-31G*	CASPT2	Exp.
11	3.81	3.71		5.21	5.27[a]	5.26[a] / 5.34[a]
12	4.84	4.70		6.08	6.04[a]	6.02[b] / 6.06[a]
13	5.11	4.98		6.52	6.00[a]	5.93[b] / 5.97[a]
14	4.47	4.37		5.86		5.23[b]
15		2.76		4.06		4.05[c]
16	2.13			3.31		3.49[c]
17	2.64		3.70	3.66		3.65[d]
18	2.59		3.80	3.74		3.74[d]
19	2.37		3.61			3.52[d]
20	2.90		4.18			3.77[d]

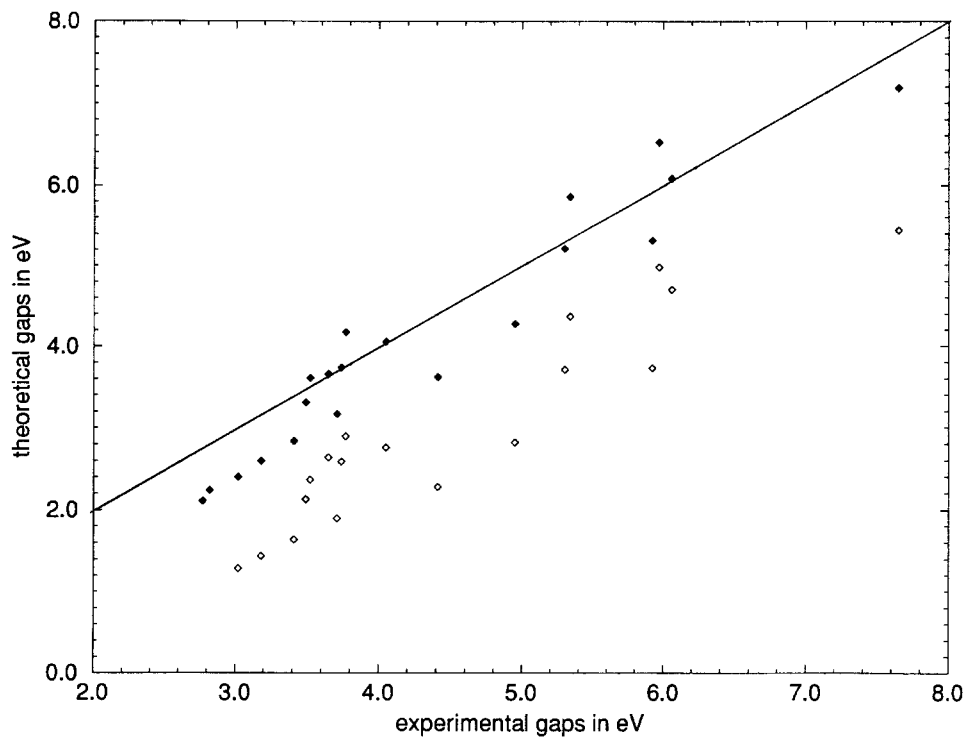[a] Ref. 6, [b] ref. 36, [c] ref. 37 and 38, [d] ref. 38.

FIGURE 4. Theoretical HOMO–LUMO gaps plotted against experimental excitation energies for **1–20** at B3LYP / CEP-31G* (filled diamonds) and SVWN (LSDA) / CEP-31G* (empty diamonds). The straight line indicates one-to-one correspondence between theory and experiment.

gies yielding IPs that are about 2.4–3.6 eV too low. Comparison between BLYP and B3LYP indicates that the use of the hybrid functional lowers the HOMO energy by up to 1.1 eV. Comparison of BVWN and BLYP data shows that the LYP correlation functional tends to raise the HOMO energy by about 1 eV, thus increasing the discrepancy with experiment. The PW91 correlation functional seems to have a similar effect as LYP, whereas P86 yields the lower HOMO energies and is thus in closest agreement with experiment of all DFT methods. The best combination of exchange and correlation

TABLE III.

Negative HOMO Energies of Polyenes at Various Theoretical Levels Using the CEP-31G* Basis Set Compared to Vertical IPs from Photoelectron Spectroscopy (in Electron Volts).

| Species	RHF	SVWN	BVWN	BLYP	BP86	B3LYP	B3LYP 6-31G*	B3P86	B3PW91	B3LYP $E_{cat-neutr}$	Exp.
C_2H_4	9.93	6.91	6.97	6.07	6.37	7.17	7.26	7.84	7.28	10.36	10.51[a]
C_4H_6	8.59	6.08	6.15	5.21	5.54	6.21	6.23	6.87	6.31	8.63	9.09[a]
C_6H_8	7.86	5.65	5.71	4.78	5.11	5.69	5.69	6.34	5.79	7.72	8.29–8.45[b]
C_8H_{10}	7.42	5.38	5.44	4.52	4.85	5.37	5.36	6.02	5.46	7.13	7.8–8.1[c]
$C_{10}H_{12}$	7.12	5.21	5.26	4.34		5.14	5.14			6.72	
$C_{12}H_{14}$	6.92	5.08	5.13	4.21		4.98	4.97	5.64		6.41	
$C_{14}H_{16}$	6.76	4.98		4.11		4.86	4.85	5.51		6.16	
$C_{16}H_{18}$	6.65	4.91	4.96	4.04	4.37	4.76	4.75	5.42	4.86	5.97	

[a] Ref. 12, [b] ref. 4, [c] ref. 3.
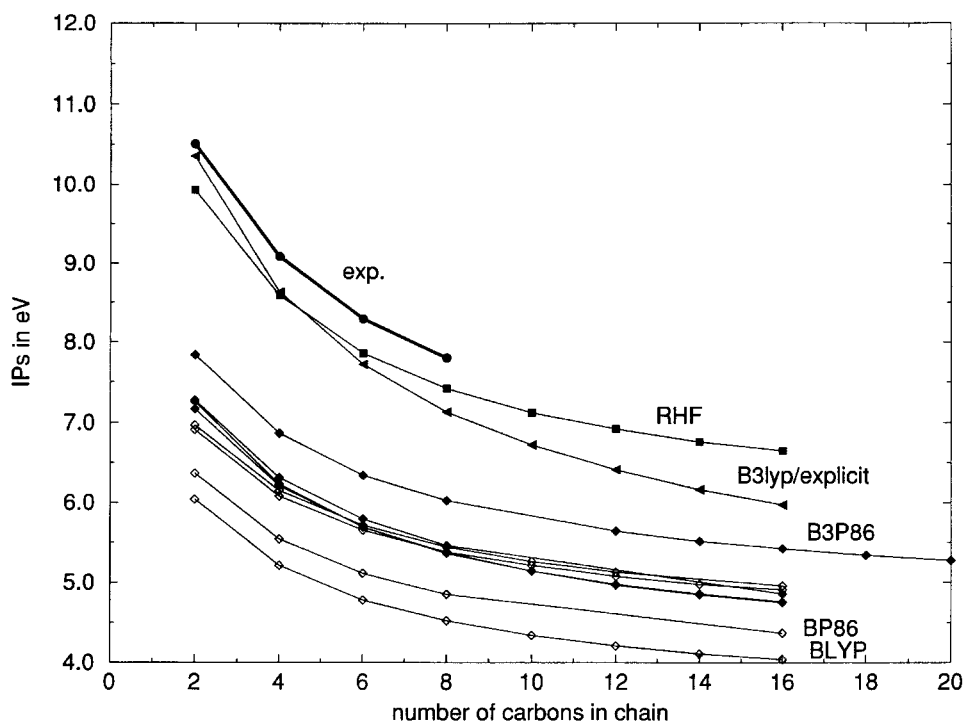
FIGURE 5. Experimental IPs and theoretical negative HOMO energies for **1–10**.

functional appears to be B3P86 which yields negative HOMO energies which are between 1.8 and 2.7 eV lower than experimental IPs.

Negative LUMO energies at various theoretical levels are listed in Table IV and are plotted in Figure 6. Experimental electron affinities are obtained as differences between experimental ionization potentials and excitation energies. All DFT methods provide LUMO energies in much closer

agreement with experimental electron affinities than RHF. SVWN and BVWN are closer to experimental values than any of the other functionals. EAs are underestimated by as little as 0.3−1.4 eV. Comparison between BLYP and B3LYP or BP86 and B3P86 shows that the use of hybrid functionals has little effect on LUMO energies especially for larger systems. For $C_{16}H_{18}$ there is virtually no difference between BP86 and B3P86 results: 3.06

TABLE IV.
Negative LUMO Energies of Polyenes at Various Theoretical Levels Using the CEP-31G* Basis Set (in Electron Volts).

Species	RHF	SVWN	BVWN	BLYP	BP86	B3LYP	B3LYP	B3P86 6-31G*	B3PW91	Exp.[a]
C_2H_4	−4.07	1.48	1.53	0.67	0.93	−0.02	−0.51	0.56	0.005	2.9
C_4H_6	−3.06	2.35	2.39	1.51	1.81	0.90	0.61	1.52	0.97	3.2
C_6H_8	−2.42	2.82	2.85	1.96	2.27	1.43	1.21	2.06	1.51	3.3−3.5
C_8H_{10}	−2.01	3.11	3.12	2.23	2.56	1.75	1.57	2.40	1.84	3.4−3.7
$C_{10}H_{12}$	−1.74	3.30	3.31	2.41		1.98	1.81			
$C_{12}H_{14}$	−1.53	3.43	3.44	2.54		2.14	1.99	2.80		
$C_{14}H_{16}$	−1.40	3.54			2.64		2.27	2.12	2.93	
$C_{16}H_{18}$	−1.29	3.62	3.61	2.72	3.06	2.36	2.23	3.03	2.47	

[a] Experimental values are obtained as differences between IPs and gaps as given in Tables I and III.
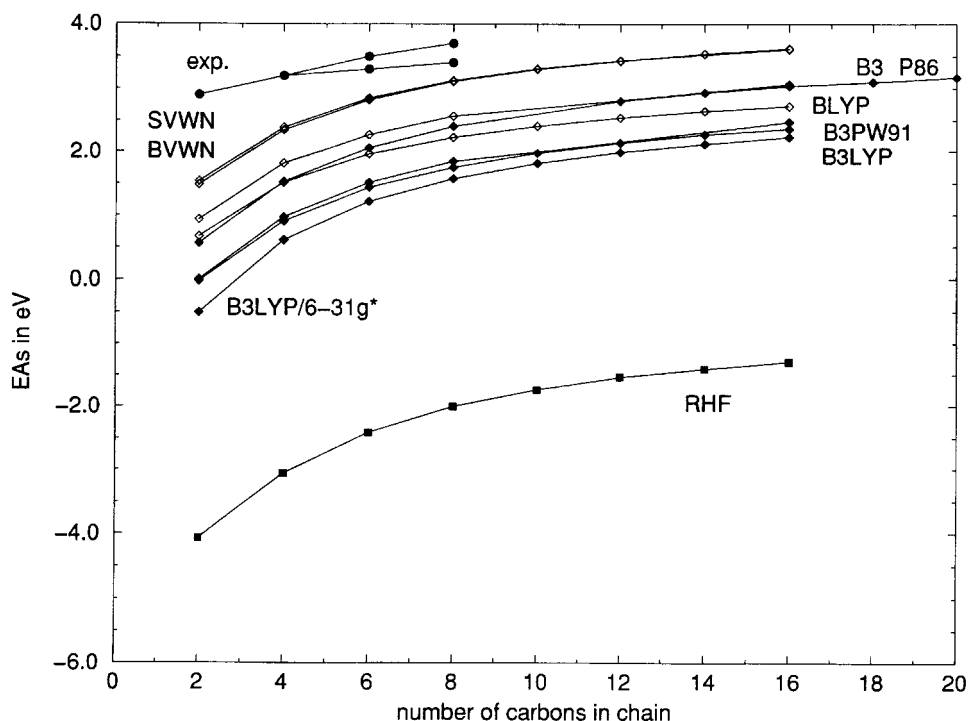
FIGURE 6. Experimental EAs and theoretical negative LUMO energies for **1–10**.

and 3.03 eV. As with the IPs, the P86 correlation functional yields data closer to experiment (0.7 eV for $C_{16}H_{18}$) than LYP and PW91. The overall error for P86 is 1.1–2.3 eV, about 1 eV larger than for SVWN and BVWN.

In conclusion, the P86 functional is superior to LYP for IPs, EAs, and band gaps. For gaps and IPs, hybrid functionals are better suited than LSDA, but for EAs LSDA leads to closest agreement with experiment. Comparison between B3LYP/CEP-31G* and B3LYP/6-31G* results shows that the use of a pseudopotential leads to small changes in gaps, IPs, and EAs compared with the changes due to the use of different functionals.

Discussion

The use of DFT eigenvalues to estimate quasi-particle energies and excitation energies has been extensively analyzed for solids and molecules.[8,9,19,20,22-24,26] The unanimous result is that there are two ways to obtain excitation energies from DFT eigenvalues. The first is to employ the HOMO–HOMO energy difference from two different calculations—one for the ground state and one for a state with fractional occupancy. The other possibility is to use the HOMO–LUMO energy

difference from a single calculation and to correct the result [eq. (3)] by the difference ($C = C_{IP} - C_{EA}$) between the derivative discontinuities $C_{IP} = \partial E_{XC}/\partial n(\mathbf{r})|_{M-\delta}$ and $C_{EA} = \partial E_{XC}/\partial n(\mathbf{r})|_{M+\delta}$ for IPs and EAs, respectively. M is the particle number of the neutral system and $\pm \delta$ designates the change in particle numbers:

$$\Delta E = IP - EA = \varepsilon_{\text{LUMO}} - \varepsilon_{\text{HOMO}} + C \quad (2)$$

To address the size of C, Godby–Schlüter–Sham[8] (GSS) calculated quasiparticle energies, LSDA band gaps, and band gaps employing the exact exchange-correlation functional for several semiconductors and diamond. LSDA and exact DFT gave similar results. Quasiparticle energies led to higher lying conduction bands than DFT and were in almost perfect agreement with experiment. The derivative discontinuity was therefore assumed to account for most of the error in the DFT band gap. It was also concluded that other functionals would not improve the DFT band gaps. Similar conclusions were reached by others.[7]

So, why do hybrid functionals predict the excitation energies of the π-systems tested here so well? Although previous studies agree that the band gap problem is due to the derivative discontinuity in the exchange correlation functional, they

come to different conclusions about whether the error is caused by too-high LUMO energies or by problems with HOMO and LUMO energies. Levy et al.[2] found that the center of the DFT band gap is given correctly. Thus HOMO and LUMO have to be too high or too low by the same amount. GSS[8] found that the LSDA valence band energy is about correct and the error in the band gap is due to a too-low-lying conduction band. In contrast, we see from Table III that with all DFT functionals, LSDA and hybrid, EAs are better estimated than IPs. SVWN (LSDA) negative LUMO energies are actually in very close agreement with EAs, whereas IPs are poor. With hybrid functionals, IPs improve by up to 1 eV but EAs become too low.

At RHF the HOMO is about correct and the error in the gaps is due to too-high-lying LUMOs. All RHF LUMOs have in fact positive energies and predict the anions to be unstable. The relationship between RHF and DFT LUMO energies and excitation energies was discussed by Malkin–Malkina–Casida–Salahub (MMCS).[30] The exact difference between ground and excited state energies at HF is given in the frozen orbital approximation as:

$$\Delta E = -\varepsilon_k + \varepsilon_a - J_{ak} + 2K_{ak} \qquad (3)$$

where ε_k is the HOMO energy, ε_a the LUMO energy, J_{ak} is the Coulomb integral, and K_{ak} the exchange integral. The corresponding expression in DFT is[8, 30]:

$$\Delta E = -\varepsilon_k + \varepsilon_a + \Delta E^{xc} \qquad (4)$$

ΔE^{xc} describes the change in exchange and correlation energy between ground and excited state. J_{ak}, K_{ak}, and ΔE^{xc} are neglected if the HOMO–LUMO gaps are used to approximate excitation energies. Hunt suggested shifting down the RHF LUMOs with a shift operator for the Coulomb term to obtain better excitation energies.[11, 30] Comparison of eqs. (3) and (4) suggests that, in DFT,

the frozen orbital approximation is less problematic than in RHF theory because no adjustment of the Coulomb energy is required.

In Table V the differences between experimental IPs and EAs and negative HOMO and LUMO energies at RHF, SVWN, B3LYP, and B3P86 are summarized for ethene through octatetraene. Δg is the difference between the errors for HOMO and LUMO and corresponds to the correction of the gap. Table V shows that, at SVWN (LSDA), the LUMOs are shifted down by about 5 eV compared to RHF and are quite close to experimental EAs. The error in the SVWN IPs is about three times as large as for the EAs. *The error in the SVWN gap is thus mainly due to underestimation of IPs rather than to overestimation of EAs.* This is in sharp contrast to results from solid state calculations where it is usually assumed that the LUMO has to be shifted up. With the hybrid functionals neither IPs nor EAs are correct but their errors are approximately equal. This leads to error cancellation when gaps are evaluated. Although Δg is equal with B3LYP and B3P86 the individual errors in the HOMO and LUMO energies differ. B3P86 yields IPs and EAs about 0.6 eV closer to experiment than B3LYP.

The dependence of Δg (the error in the gap) on the exchange correlation functional suggests that eq. (2) is incomplete. A second error seems to be present which we designate $\Delta\varepsilon$ [eq. (6)] in addition to C, the derivative discontinuity, which is assumed to be independent of the functional[8, 22, 26]:

$$\Delta E = \text{IP} - \text{EA} = \varepsilon_{\text{LUMO}} - \varepsilon_{\text{HOMO}} + \Delta\varepsilon + C \quad (5)$$

If C were indeed solely responsible for the band gap error at LSDA, then, in going from LSDA to hybrid functionals, $\Delta\varepsilon$ would have to increase just enough to partially cancel C. We think that it is much more likely that the error in the LSDA gap is, to a significant extent, due to deficiencies in the functionals and that C is much smaller than assumed so far. C, as defined above, results as the

TABLE V.
Differences Between Theoretical and Experimental IPs and EAs and Δg is the Correction to the Gap for Selected Theoretical Levels (See Text).

Species	RHF			SVWN			B3LYP			B3P86		
	ΔIP	ΔEA	Δg	ΔIP	ΔEA	Δg	ΔIP	ΔEA	Δg	ΔIP	ΔEA	Δg
C_2H_4	0.6	7.0	6.4	3.6	1.4	−2.2	3.3	2.9	−0.5	2.7	2.3	−0.4
C_4H_6	0.5	6.3	5.7	3.0	0.9	−2.2	2.9	2.3	−0.6	2.2	1.7	−0.6
C_6H_8	0.4	6.5	5.3	2.6	0.5	−2.1	2.6	1.9	−0.7	2.0	1.2	−0.7
C_8H_{10}	0.4	5.4	5.0	2.4	0.3	−2.1	2.4	1.7	−0.8	1.8	1.1	−0.8

difference between derivative discontinuities with respect to particle numbers for IPs and EAs. Excitation of electrons, however, does not involve a change in particle number. The problem arises because the excitation energies are obtained as differences between IPs and EAs and because these are not calculated explicitly but crudely approximated as negative HOMO and LUMO energies. Two errors are thus introduced one for the IP and one for the EA. Both errors are most likely substantial. What affects the gap, however, is the difference between the two. This difference might in fact be small because *both* C_{IP} and C_{EA} involve changes in exchange correlation for systems which differ by exactly one electron and should thus be of comparable size. Especially for larger systems this assumption seems to be very reasonable.

Moreover, the above argument is consistent with the fact that DFT energy gaps with hybrid functionals are in close agreement with experimental excitation energies, while IPs and EAs are vertically shifted by roughly the same amount (2–3 eV). The improvement achieved with the hybrid functional therefore appears to be that an unknown error in LSDA, which differs in size for IPs and EAs, has been removed. What remains is a contribution that still depends on the functional but is about the same size for IPs and EAs. Discrepancies between our data and solid state results are not likely due to differences between finite and infinite systems because it was shown that the problems with the derivative discontinuity for calculation of excitation energies and band gaps are analogous.[22]

Conclusions

HOMO–LUMO energy differences with DFT hybrid functionals yield excitation energies in good agreement with experimental values for 20 randomly selected π-systems. Negative HOMO energies and negative LUMO energies are too low compared to experimental IPs and EAs. These findings are consistent with the assumption that good gaps are due to partial cancellation of the particle-number derivative discontinuities in the exchange-correlation functional associated with IPs and EAs. However, other factors might be at work and the problem has to be further investigated.

Although previous theoretical analyses predicted that band gaps will not improve in going beyond LSDA, we show here that DFT hybrid methods lead to significant improvement of the gaps. Furthermore, individual HOMO and LUMO levels depend strongly on the functional. This indicates that there might be room for improving the functionals further. Studies employing half/half functionals that include more Hartree–Fock exchange are underway. The possibility that the improvement is due to fortuitous error cancellation has to be investigated.

We hope that this contribution will restimulate the discussion of the ''band gap problem'' on a more positive note. If the agreement between DFT/hybrid HOMO–LUMO energy differences and experimental excitation energies turns out to hold, in general, and transfers to solid-state calculations, an enormous improvement of band structure calculations could be achieved with only a moderate increase of computational cost.

Acknowledgments

References

1. G. Brocks and A. Tol, *J. Phys. Chem.*, **100**, 1838 (1996).

2. R. Hoffmann, C. Janiak, and C. Kollmar, *Macromolecules*, **24**, 3725 (1991).

3. R. J. Cave and E. R. Davidson, *J. Phys. Chem.*, **92**, 2173 (1988).

4. R. J. Cave and E. R. Davidson, *J. Phys. Chem.*, **92**, 614 (1988).

5. T. Hashimoto, H. Nakano, and K. Hirao, *J. Chem. Phys.*, **104**, 6244 (1996).

6. H. Nakano, T. Tsuneda, T. Hashimoto, and K. Hirao, *J. Chem. Phys.*, **104**, 2312 (1996).

7. R. M. Dreizler and E. K. U. Gross, *Density Functional Theory*, Springer, Berlin, 1990.

8. R. W. Godby, M. Schlüter, and L. J. Sham, *Phys. Rev. B*, **37**, 10159 (1988).

9. L. Fritsche, *Physica B*, **172**, 7 (1991).

10. M. P. Keane, A. Naves de Brito, N. Correira, S. Svensson, L. Karlsson, B. Wannberg, U. Gelius, S. Lunell, W. R. Salaneck, M. Lögdlund, D. B. Swanson, and A. G. MacDiarmid, *Phys. Rev. B*, **45**, 6390 (1992).

11. W. J. Hunt and A. Goddard III, *Chem Phys. Lett.*, **3**, 414 (1969).

12. K. Kimura, S. Katsumata, Y. Achiba, T. Yamazaki, and S. Iwata, *Handbook of HeI Photoelectron Spectra of Fundamental Organic Molecules*, Halsted Press, New York, 1981.

13. R. Stumpf and M. Scheffler, *Comp. Phys. Commun.*, **79**, 447 (1994).

14. G. Brocks, P. J. Kelly, and R. Car, *Synth. Met.*, **55–57**, 4243 (1993).

15. J. Paldus and E. Chin, *Int. J. Quant. Chem.*, **24**, 373 (1983).

16. J. Paldus, E. Chin, and M. G. Grey, *Int. J. Quant. Chem.*, **24**, 397 (1983).

17. R. Pauncz and J. Paldus, *Int. J. Quant. Chem.*, **24**, 411 (1983).

18. J.-L. Brédas In *Handbook of Conducting Polymers*, T. A. Skotheim, Ed., Marcel Dekker, New York, 1986, p. 859.

19. R. K. Nesbet, *J. Phys. Chem.*, **100**, 6104 (1996).

20. J. F. Janak, *Phys. Rev. B*, **18**, 7165 (1978).

21. J. Callaway and N. H. March, *Solid State Phys.*, **38**, 135 (1984).

22. M. Levy, *Phys. Rev. A*, **52**, 50 (1995).

23. E. K. U. Gross, L. N. Oliveira, and W. Kohn, *Phys. Rev. A*, **37**, 2805 (1988).

24. E. K. U. Gross, L. N. Oliveira, and W. Kohn, *Phys. Rev. A*, **37**, 2809 (1988).

25. L. N. Oliveira, E. K. U. Gross, and W. Kohn, *Phys. Rev. A*, **37**, 2821 (1988).

26. J. P. Perdew and M. Levy, *Phys. Rev. Lett.*, **51**, 1884 (1983).

27. P. G. Parr and W. Yang *Density-Functional Theory of Atoms and Molecules*, Oxford University Press, New York, 1989.

28. M. J. Frisch, A. E. Frisch, and J. B. Foresman *Gaussian 94 User's Reference*, Gaussian, Inc., Pittsburgh, PA, 1994–1995.

29. M. J. Frisch, G. W. Trucks, H. B. Schlegel, P. M. W. Gill, B. G. Johnson, M. A. Robb, J. R. Cheeseman, T. Keith, G. A. Petersson, J. A. Montgomery, K. Raghavachari, M. A. Al-Laham, V. G. Zakrzewski, J. V. Ortiz, J. B. Foresman, C. Y. Peng, P. Y. Ayala, W. Chen, M. W. Wong, J. L. Andres, E. S. Replogle, R. Gomperts, R. L. Martin, D. J. Fox, J. S. Binkley, D. J. Defrees, J. Baker, J. P. Stewart, M. Head-Gordon, C. Gonzalez, and J. A. Pople, *Gaussian-94*, Gaussian, Inc., Pittsburgh, PA, 1995.

30. V. G. Malkin, O. L. Malkina, M. E. Casida, and D. R. Salahub, *J. Am. Chem. Soc.*, **116**, 5898 (1994).

31. A. J. Merer and R. S. Mulliken, *Chem. Rev.*, **69**, 639 (1969).

32. O. A. Mosher, W. M. Flicker, and A. Kuppermann, *J. Chem. Phys.*, **59**, 6502 (1973).

33. W. M. Flicker, O. A. Mosher, and A. Kuppermann, *Chem. Phys. Lett.*, **45**, 492 (1977).

34. J. Gavin, R. M. C. Weisman, J. K. McVey, and S. A. Rice, *J. Chem. Phys.*, **68**, 522 (1978).

35. W. Kutzelnigg, *Einführung in die Theoretische Chemie, Band 2*, Verlag Chemie, Weinheim, 1978.

36. *Sadler Handbook of Ultraviolet Spectra*; Sadler Research Laboratories, Philadelphia, PA, 1979.

37. R. Colditz, D. Grebner, M. Helbig, and S. Rentsch, *Chem. Phys.*, **201**, 309 (1995).

38. I. H. Jenkins, U. Salzner, and P. G. Pickup, *Chem. Mat.*, **8**, 1444 (1996).